

## Research Article

# Correlation-Based Amplitude Estimation of Coincident Partial in Monaural Musical Signals

Jayme Garcia Arnal Barbedo<sup>1</sup> and George Tzanetakis<sup>2</sup>

<sup>1</sup>Department of Communications, FEEC, UNICAMP C.P. 6101, CEP: 13.083-852, Campinas, SP, Brazil

<sup>2</sup>Department of Computer Science, University of Victoria, Columbia, Canada V8W 3P6

Correspondence should be addressed to Jayme Garcia Arnal Barbedo, jbarbedo@gmail.com

Received 12 January 2010; Revised 29 April 2010; Accepted 5 July 2010

Academic Editor: Mark Sandler

Copyright © 2010 J. G. A. Barbedo and G. Tzanetakis. This is an open access article distributed under the Creative Commons Attribution License, which permits unrestricted use, distribution, and reproduction in any medium, provided the original work is properly cited.

This paper presents a method for estimating the amplitude of coincident partials generated by harmonic musical sources (instruments and vocals). It was developed as an alternative to the commonly used interpolation approach, which has several limitations in terms of performance and applicability. The strategy is based on the following observations: (a) the parameters of partials vary with time; (b) such a variation tends to be correlated when the partials belong to the same source; (c) the presence of an interfering coincident partial reduces the correlation; and (d) such a reduction is proportional to the relative amplitude of the interfering partial. Besides the improved accuracy, the proposed technique has other advantages over its predecessors: it works properly even if the sources have the same fundamental frequency, it is able to estimate the first partial (fundamental), which is not possible using the conventional interpolation method, it can estimate the amplitude of a given partial even if its neighbors suffer intense interference from other sources, it works properly under noisy conditions, and it is immune to intraframe permutation errors. Experimental results show that the strategy clearly outperforms the interpolation approach.

## 1. Introduction

The problem of source separation of audio signals has received increasing attention in the last decades. Most of the effort has been devoted to the determined and overdetermined cases, in which there are at least as many sensors as sources [1–4]. These cases are, in general, mathematically more treatable than the underdetermined case, in which there are fewer sensors than sources. However, most real-world audio signals are underdetermined, many of them having only a single channel. This has motivated a number of proposals dealing with this kind of problem. Most of such proposals try to separate speech signals [5–9], speech from music [10–12], or a singing voice from music [13]. Only recently methods trying to deal with the task of separating different instruments in monaural musical signals have been proposed [14–18].

One of the main challenges faced in music source separation is that, in real musical signals, simultaneous sources (instruments and vocals) normally have a high degree of

correlation and overlap both in time and frequency, as a result of the underlying rules normally followed by western music (e.g., notes with integer ratios of pitch intervals). The high degree of correlation prevents many existing statistical methods from being used, because those normally assume that the sources are statistically independent [14, 15, 18]. The use of statistical tools is further limited by the also very common assumption that the sources are highly disjoint in the time–frequency plane [19, 20], which does not hold when the notes are harmonically related.

An alternative that has been used by several authors is the sinusoidal modeling [21–23], in which the signals are assumed to be formed by the sum of a number of sinusoids whose parameters can be estimated [24].

In many applications, only the frequency and amplitude of the sinusoids are relevant, because the human hearing is relatively insensitive to the phase [25]. However, estimating the frequency in the context of musical signals is often challenging, since the frequencies do not remain steady with time, especially in the presence of vibrato, which manifests

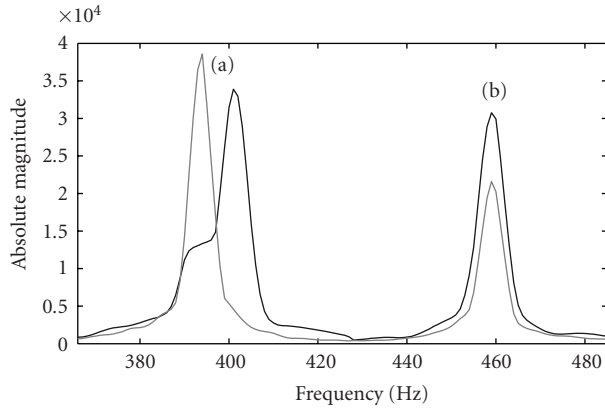


FIGURE 1: Magnitude spectrum showing: (a) an example of partially colliding partials, and (b) an example of coincident partials.

as frequency and amplitude modulation. Using very short time windows to perform the analysis over a period in which the frequencies would be expected to be relatively steady also does not work, as this procedure results in a very coarse frequency resolution due to the well-known time-frequency tradeoff. The problem is even more evident in the case of coincident partials, because different partials vary in different ways around a common frequency, making it nearly impossible to accurately estimate their frequencies. However, in most cases the band within which the partials are located can be determined instead. Since the phase is usually ignored and the frequency often cannot be reliably estimated due to the time variations, it is the amplitude of individual partials that can provide the most useful information to efficiently separate coincident partials.

For the remainder of this paper, the term *partial* will refer to a sinusoid with a frequency that varies with time. As a result, the frequency band occupied by a partial during a period of time will be given by the range of such a variation. It is also important to note that the word *partial* can be both used to indicate part of an individual source (isolated harmonic), or part of the whole mixture—in this case, the merging of two or more coincident partials would also be called a partial. Partial referring to the mixture will be called *mixture partials* whenever the context does not resolve this ambiguity.

The sinusoidal modeling technique can successfully estimate the amplitudes when the partials of different sources do not collide, but it loses its effectiveness when the frequencies of the partials are close. The expression colliding partials refers here to the cases in which two partials share at least part of the spectrum (Figure 1(a)). The expression coincident partials, on the other hand, is used when the colliding partials are mostly concentrated in the same spectral band (Figure 1(b)). In the first case, the partials may be separated enough to generate some effects that can be explored to resolve them, but in the second case they usually merge in such a way they act as a single partial. In this work, two partials will be considered coincident if their frequencies are separated by less than 5% for frequencies below 500 Hz, and

by less than 25 Hz for frequencies above 500 Hz—according to tests carried out previously, those values are roughly the thresholds for which traditional techniques to resolve close sinusoids start to fail. A small number of techniques to resolve colliding partials have been proposed, and only a few of them can deal with coincident partials.

Most techniques proposed in the literature can only reliably resolve colliding partials if they are not coincident. Klapuri et al. [26] explore the amplitude modulation resulting from two colliding partials to resolve their amplitudes. If more than two partials collide, the standard interpolation approach as described later is used instead. Virtanen and Klapuri [27] propose a technique that iteratively estimates phases, amplitudes, and frequencies of the partials using a least-square solution. Parametric approaches like this one tend to fail when the partials are very close, because some of the matrices used to estimate the parameters tend to become singular. The same kind of problem can occur in the strategy proposed by Tolonen [16], which uses a nonlinear least-squares estimation to determine the sinusoidal parameters of the partials. Every and Szymanski [28] employ three filter designs to separate partly overlapping partials. The method does not work properly when the partials are mostly concentrated in the same band. Hence, it cannot be used to estimate the amplitudes of coincident or almost coincident partials.

There are a few proposals that are able to resolve coincident partials, but they only work properly under certain conditions. An efficient method to separate coincident partials based on the similarity of the temporal envelopes was proposed by Viste and Evangelista [29], but it only works for multichannel mixtures. Duan et al. [30] use an average harmonic structure (AHS) model to estimate the amplitudes of coincident partials. To work properly, this method requires that, at least for some frames, the partials be sufficiently disjoint so their individual features can be extracted. Also, the technique does not work when the frequencies of the sources have octave relations. Woodruff et al. [31] propose a technique based on the assumptions that harmonics of the same source have correlated amplitude envelopes and that phase differences can be predicted from the fundamental frequencies. The main limitation of the technique is that it depends on very accurate pitch estimates.

Since most of these elaborated methods usually have limited applicability, simpler and less constrained approaches are often adopted instead. Some authors simply attribute all the content to a single source [32], while others use a simple interpolation approach [33–35]. The interpolation approach estimates the amplitude of a given partial that is known to be colliding with another one by linearly interpolating the amplitudes of other partials belonging to the same source. Several partials can be used in such an interpolation but, according to Virtanen [25], normally only the two adjacent ones are used, because they tend to be more correlated to the amplitude of the overlapping partial. The advantage of such a simple approach is that it can be used in almost every case, with the only exceptions being those in which the sources have the same fundamental frequency. On the other hand, it has three main shortcomings: (a) it assumes

that both adjacent partials are not significantly changed by the interference of other sources, which is often not true; (b) the first partial (fundamental) cannot be estimated using this procedure, because there is no previous partial to be used in the interpolation; (c) the assumption that the interpolation of the partials is a good estimate only holds for a few instruments and, for the cases in which a number of partials are practically nonexistent, such as a clarinet with odd harmonics, the estimates can be completely wrong.

This paper presents a more refined alternative to the interpolation approach, using some characteristics of the harmonic audio signals to provide a better estimate for the amplitudes of coincident partials. The proposal is based on the hypothesis that the frequencies of the partials of a given source will vary in approximately the same fashion over time. In a short description, the algorithm tracks the frequency of each mixture partial over time, and then uses the results to calculate the correlations among the mixture partials. The results are used to choose a reference partial for each source, by determining which is the mixture partial that is more likely to belong exclusively to that source, that is, the partial with minimum interference from other sources. The influence of each source over each mixture partial is then determined by the correlation of the mixture partials with respect to the reference partials. Finally, this information is used to estimate how the amplitude of each mixture partial should be split among its components.

This proposal has several advantages over the interpolation approach.

- (a) Instead of relying in the assumption that both neighbor partials are interference-free, the algorithm depends only on the existence of one partial strongly dominated by each source to work properly, and relatively reliable estimates are possible even if this condition is not completely satisfied.
- (b) The algorithm works even if the sources have the same fundamental frequency ( $F_0$ )—tests comparing the spectral envelopes of a large number of pairs of instruments playing the same note and having the same RMS level, revealed that in 99.2% of the cases there was at least one partial whose energy was more than five times greater than the energy of its counterpart.
- (c) The first partial (fundamental) can be estimated.
- (d) There are no intraframe permutation errors, meaning that, assuming the amplitude estimates within a frame are correct, they will always be assigned to the correct source.
- (e) The estimation accuracy is much greater than that achieved by the interpolation approach.

In the context of this work, the term *source* refers to a sound object with harmonic frequency structure. Therefore, a vocal or an instrument generating a given note is considered a source. This also means that the algorithm is not able to deal with sound sources that do not have harmonic characteristics, like percussion instruments.

The paper is organized as follows. Section 2 presents the preprocessing. Section 3 describes all steps of the algorithm. Section 4 presents the experiments and corresponding results. Finally, Section 5 presents the conclusions and final remarks.

## 2. Preprocessing

Figure 2 shows the basic structure of the algorithm. The first three blocks, which represent the preprocessing, are explained in this section. The last four blocks represent the core of the algorithm and are described in Section 3. The preprocessing steps described in the following are fairly standard and have shown to be adequate for supporting the algorithm.

*2.1. Adaptive Frame Division.* The first step of the algorithm is dividing the signal into frames. This step is necessary because the amplitude estimation is made in a frame-by-frame basis. The best procedure here is to set the boundaries of each frame at the points where an onset [36, 37] (new note, instrument or vocal) occurs, so the longest homogeneous frames are considered. The algorithm works better if the onsets themselves are not included in the frame, because during the period they occur, the frequencies may vary wildly, interfering with the partial correlation procedure described in Section 3.3. The algorithm presented in this paper does not include an onset-detection procedure in order to avoid cascaded errors, which would make it more difficult to analyze the results. However, a study about the effects of onset misplacements on the accuracy of the algorithm is presented in Section 4.5.

To cope with partial amplitude variations that may occur within a frame, the algorithm includes a procedure to divide the original frame further, if necessary. The first condition for a new division is that the duration of the note be at least 200 ms, since dividing shorter frames would result in frames too small to be properly analyzed. If this condition is satisfied, the algorithm divides the original frame into two frames, the first one having a 100-ms length, and the second one comprising the remainder of the frame. The algorithm then measures the RMS ratio between the frames according to

$$R_{\text{RMS}} = \frac{\min(r_1, r_2)}{\max(r_1, r_2)}, \quad (1)$$

where  $r_1$  and  $r_2$  are the RMS of the first and second new frames, respectively.  $R_{\text{RMS}}$  will always assume a value between zero and one. The RMS values were used here because they are directly related to the actual amplitudes, which are unknown at this point.

The  $R_{\text{RMS}}$  value is then stored and a new division is tested, now with the first new frame being 105-ms long and the second being 5 ms shorter than it was originally. This new  $R_{\text{RMS}}$  value is stored and new divisions are tested by successively increasing the length of the first frame by 5 ms and reducing the second one by 5 ms. This is done until the

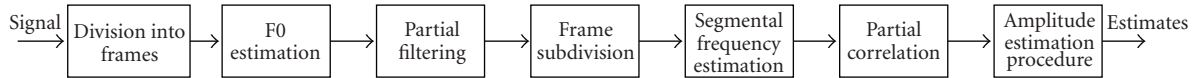


FIGURE 2: Algorithm general structure.

resulting second frame is 100-ms long or shorter. If the lowest  $R_{RMS}$  value obtained is below 0.75 (empirically determined), this indicates a considerable amplitude variation within the frame, and the original frame is definitely divided accordingly. If, as a result of this new division, one or both the new frames have a length greater than 200 ms, the procedure is repeated and new divisions may occur. This is done until all frames are smaller than 200-ms, or until all possible  $R_{RMS}$  values are above 0.75.

Some results using different fixed frame lengths are presented in Section 4.

**2.2. F0 Estimation and Partial Location.** The position of the partials of each source is directly linked to their fundamental frequency (F0). The first versions of the algorithm included the multiple fundamental frequencies estimator proposed by Klapuri [38]. A common consequence of using supporting tools in an algorithm is that the errors caused by flaws inherent to those supporting tools will propagate throughout the rest of the algorithm. Fundamental frequency errors are indeed a problem in the more general context of sound source separation, but since the scope of this paper is limited to the amplitude estimation, errors coming from third-party tools should not be taken into account in order to avoid contamination of the results. On the other hand, if all information provided by the supporting tools is assumed to be known, all errors will be due to the proposed algorithm, providing a more meaningful picture of its performance. Accordingly, it is assumed that a hypothetical sound source separation algorithm would eventually reach a point in which the amplitude estimation would be necessary—to reach this point, such an algorithm would maybe depend on a reliable F0 estimator, but this is a problem that does not concern this paper, so the correct fundamental frequencies are assumed to be known.

Although F0 errors are not considered in the main tests, it is instructive to discuss some of the impacts that F0 errors would have in the algorithm proposed here. Such a discussion is presented in the following, and some practical tests are presented in Section 4.6.

When the fundamental frequency of a source is misestimated, the direct consequence is that a number of false partials (partials that do not exist in the actual signal, but that are detected by the algorithm due to F0 estimation error) will be considered and/or a number of real partials will be ignored. F0 errors may have significant impact in the estimation of the amplitudes of correct partials depending on the characteristics of the error. Higher octave errors, in which the detected F0 is actually a multiple of the correct one, have very little impact on the estimation of correct partials. This is because that, in this case, the algorithm will ignore

a number of partials, but those that are taken into account are actual partials. Problems may arise when the algorithm considers false partials, which can happen both in the case of lower octave errors, in which the detected F0 is a submultiple of the correct one, and in the case of nonoctave errors—this last situation is the worst because most considered partials are actually false, but fortunately this is the less frequent kind of error. When the positions of those false partials coincide with the positions of partials belonging to sources whose F0 were correctly identified, some problems may happen. As will be seen in Section 3.4, the proposed amplitude estimation procedure depends on the proper choice of reference partials for each instrument, which are used as a template to estimate the remaining ones. If the first reference partial to be chosen belongs to the instrument for which the F0 was misestimated, that has little impact on the amplitude estimation of the real partials. On the other hand, if the first reference partial belongs to the instrument with the correct F0, then the entire amplitude estimation procedure may be disrupted. The reasons for this behavior are presented in Section 4.6, together with some results that illustrate how serious is the impact of such a situation over the algorithm performance.

The discussion above is valid for significant F0 estimation errors—precision errors, in which the estimated frequency deviates by at most a few Hertz from the actual value, are easily compensated by the algorithm as it uses a search width of  $0.1 \cdot F0$  around the estimated frequency to identify the correct position of the partial.

As can be seen, considerable impact on the proposed algorithm will occur mostly in the case of lower octave errors, since they are relatively common and result in a number of false partials—a study about this impact is presented in Section 4.6.

To work properly, the algorithm needs a good estimate of where each partial is located—the location or position of a partial, in the context of this work, refers to the central frequency of the band occupied by that partial (see definition of partial in the introduction). Simply, taking multiples of F0 sometimes work, but the inherent inharmonicity [39, 40] of some instruments may cause this approach to fail, especially if one needs to take several partials into consideration. To make the estimation of each partial frequency more accurate, an algorithm was created—the algorithm is fed with the frames of the signal and it outputs the position of the partials. The steps of the algorithm for each F0 are the following:

- (a) The expected (preliminary) position of each partial ( $p_n$ ) is given by  $p_{n-1} + F0$ , with  $p_0 = 0$ .
- (b) The short-time discrete Fourier transform (STDFT) is calculated for each frame, from which the magnitude spectrum  $M$  is extracted.

- (c) The adjusted position of the current partial ( $\hat{p}_n$ ) is given by the highest peak in the interval  $[p_n - s_w, p_n + s_w]$  of  $M$ , where  $s_w = 0.1 \cdot F_0$  is the search width. This search width contains the correct position of the partial in nearly 100% of the cases; a broader search region was avoided in order to reduce the chance of interference from other sources. If the position of the partial is less than  $2s_w$  apart from any partial position calculated previously for other source, and they are not coincident (less than 5% or 25 Hz apart), the positions of both partials are recalculated considering  $s_w$  equal to half the frequency distance among the two partials.

When two partials are coincident in the mixed signal, they often share the same peak, in which case steps (a) to (c) will determine not their individual positions, but their combined position, which is the position of the mixture partial. Sometimes coincident partials may have discernible separate peaks; however, they are so close that the algorithm can take the highest one as the position of the mixture partial without problem. After the positions of all partials related to all fundamental frequencies have been estimated, they are grouped into one single set containing the positions of all mixture partials. The procedure described in this section has led to partial frequency estimates that are within 5% from the correct value (inferred manually) in more than 90% of the cases, even when a very large number of partials are considered.

**2.3. Partial Filtering.** The mixture partials for which the amplitudes are to be estimated are isolated by means of a filterbank. In real signals, a given partial usually occupies a certain band of the spectrum, which can be broader or narrower depending on a number of factors like instrument, musician, and environment, among others. Therefore, a filter with a narrow pass-band may be appropriate for some kinds of sources, but may ignore relevant parts of the spectrum for others. On the other hand, a broad pass-band will certainly include the whole relevant portion of the spectrum, but may also include spurious components resulting from noise and even neighbor partials. Experiments have indicated that the most appropriate band to be considered around the peak of a partial is given by the interval  $[0.5 \cdot (p_{n-1} + p_n), 0.5 \cdot (p_n + p_{n+1})]$ , where  $p_n$  is the frequency of the partial under analysis, and  $p_{n-1}$  and  $p_{n+1}$  are the frequencies of the closest partials with lower and higher frequencies, respectively.

The filterbank used to isolate the partials is composed by third-order elliptic filters, with a passband ripple of 1 dB and stopband attenuation of 80 dB. This kind of filter was chosen because of its steep rolloff. Finite impulse response (FIR) filters were also tested, but the results were practically the same, with a considerably greater computational complexity.

As commented before, this method is intended to be used in the context of sound source separation, whose main objective is to resynthesize the sources as accurately as possible. Estimating the amplitudes of coincident partials is an important step toward such an objective, and ideally the amplitudes of all partials should be estimated. In practice,

however, when partials have very low energy, noise plays an important role, making it nearly impossible to extract enough information to perform a meaningful estimate. As a result of those observations, the algorithm only takes into account partials whose energy—obtained by the integration of the power spectrum within the respective band—is at least 1% of the energy of the most energetic partial. Mixture partials follow the same rules; that is, they will be considered only if they have at least one percent of the energy the strongest partial—thus, the energy of an individual partial in a mixture may be below the 1% limit. It is important to notice that partials below  $-20$  dB from the strongest one may, in some cases, be relevant. Such a hard lower limit for the partial energy is the best current solution for the problem of noisy partials, but alternative strategies are currently under investigation. In order to avoid that a partial be considered in certain frames and not in others, if a given  $F_0$  keeps the same in consecutive frames, the number of partials considered by the algorithm is also kept the same.

### 3. The Proposed Algorithm

**3.1. Frame Subdivision.** The resulting frames after the filtering are subdivided into 10-ms subframes, with no overlap (overlapping the sub-frames did not improve the results). Longer sub-frames were not used because they may not provide enough points for the subsequent correlation calculation (see Section 3.3) to produce meaningful results. On the other hand, if the sub-frame is too short and the frequency is low, only a fraction of a period may be considered in the frequency estimation described in Section 3.2, making such estimation either unreliable, or even impossible.

**3.2. Partial Trajectory Estimation.** The frequency of each partial is expected to fluctuate over the analysis frame, which have a length of at least 100 ms. Also, it is expected that partials belonging to a given source will have similar frequency trajectories, which can be explored to match partials to that particular source. The 10-ms sub-frames resulting from the division described in Section 3.1 are used to estimate such a trajectory. The frequency estimation for each 10-ms sub-frame is performed in the time domain by taking the first and last zero-crossing, measuring the distance  $d$  in seconds and the number of cycles  $c$  between those zero-crossings, and then determining the frequency according to  $f = c/d$ . The exact position of the zero-crossing is given by

$$z_c = p_1 + \frac{|a_1| \cdot (p_2 - p_1)}{|a_1| + |a_2|}, \quad (2)$$

where  $p_1$  and  $p_2$  are, respectively, the positions in seconds of the samples immediately before and immediately after the zero-crossing, and  $a_1$  and  $a_2$  are the amplitudes of those same samples. Once the frequencies for each 10-ms sub-frame are calculated, they are accumulated into a partial trajectory.

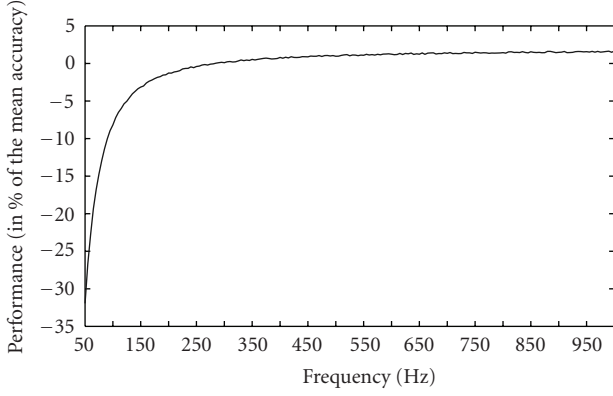


FIGURE 3: Effect of the frequency on the accuracy of the amplitude estimates.

It is worth noting that there are more accurate techniques to estimate a partial trajectory, like the normalized cross-correlation [41]. However, replacing the zero-crossing approach by the normalized cross-correlation resulted in almost the same overall amplitude estimation accuracy (mean error values differ by less than 1%), probably due to artificial fluctuations in the frequency trajectory that are introduced by the zero-crossing approach. Therefore, any of the approaches can be used without significant impact on the accuracy. The use of the zero-crossings, in this context, is justified by the low computational complexity associated.

The use of sub-frames as small as 10-ms has some important implications in the estimation of low frequencies. Since at least two zero-crossings are necessary for the estimates, the algorithm cannot deal with frequencies below 50 Hz. Also, below 150 Hz the partial trajectory shows some fluctuations that may not be present in higher frequency partials, thus reducing the correlation between partials and, as a consequence, the accuracy of the algorithm. Figure 3 shows the effect of the frequency on the accuracy of the amplitude estimates. In the plot, the vertical scale indicates how better or worse is the performance for that frequency with respect to the overall accuracy of the accuracy, in percentage. As can be seen, for 100 Hz the accuracy of the algorithm is 16% below average, and the accuracy drops rapidly as lower frequencies are considered. However, as will be seen in Section 4, the accuracy for such low frequencies is still better than that achieved by the interpolation approach.

**3.3. Partial Trajectory Correlation.** The frequencies estimated for each sub-frame are arranged into a vector, which generates trajectories like those shown in Figure 4. One trajectory is generated for each partial. The next step is to calculate the correlation between each possible pair of trajectories, resulting in  $N(N-1)/2$  correlation values, where  $N$  is the number of partials.

**3.4. Amplitude Estimation Procedure.** The main hypothesis motivating the procedure described here is that the partial frequencies of a given instrument or vocal vary approximately in the same way with time. Therefore, it is

hypothesized that the correlation between the trajectories of two mixture partials will be high when they both belong exclusively to a single source, with no interference from other partials. Conversely, the lowest correlations are expected to occur when the mixture partials are completely related to different sources. Finally, when one partial results from a given source  $A$  (called reference), and the other one results from the merge of partials coming both from source  $A$  and from other sources  $S$ , intermediary correlation values are expected. More than that, it is assumed that the correlation values will be proportional to the ratio  $a_A/a_S$  in the second mixture partial, where  $a_A$  is the amplitude of source  $A$  partial and  $a_S$  is the amplitude of the mixture partial with the source  $A$  partial removed. If  $a_A$  is much larger than  $a_S$ , it is said that the partial from source  $A$  dominates that band.

**Lemma 1.** *Let  $A_1 = X_1 + N_1$  and  $A_2 = X_2 + N_2$  be independent random variables, and let  $A_3 = aA_1 + bA_2$  be a random variable representing their weighted sum. Also, let  $X_1, X_2$  also be independent random variables, and  $N_1$  and  $N_2$  be zero-mean independent random variables. Finally, let*

$$\rho_{X,Y} = \frac{\text{cov}(X, Y)}{\sigma_X \sigma_Y} = \frac{E((X - \mu_X)(Y - \mu_Y))}{\sigma_X \sigma_Y} \quad (3)$$

be the correlation coefficient between two random variables  $X$  and  $Y$  with expected values  $\mu_X$  and  $\mu_Y$  and standard deviations  $\sigma_X$  and  $\sigma_Y$ . Then,

$$\frac{\rho_{A_1, A_3}}{\rho_{A_2, A_3}} = \frac{a}{b} \left( \frac{\sigma_{X_1}^2 + \sigma_{N_1}^2}{\sigma_{X_2}^2 + \sigma_{N_2}^2} \right) \left( \frac{\sqrt{\sigma_{X_2}^2 + \sigma_{N_2}^2}}{\sqrt{\sigma_{X_1}^2 + \sigma_{N_1}^2}} \right). \quad (4)$$

Assuming that  $\sigma_{N_1}^2 \ll \sigma_{X_1}^2$ ,  $\sigma_{N_2}^2 \ll \sigma_{X_2}^2$ , and  $\sigma_{X_1} \equiv \sigma_{X_2}$ , (4) reduces to

$$\frac{\rho_{A_1, A_3}}{\rho_{A_2, A_3}} = \frac{a}{b}. \quad (5)$$

For proof, see the appendix.

The lemma stated above can be directly applied to the problem presented in this paper, as explained in the following. First, a model is defined in which the  $n$ th partial  $P_n$  of an instrument is given by  $P_n(t) = n \cdot F_0(t)$ , where  $F_0(t)$  is the time-varying fundamental frequency and  $t$  is the time index. In this idealized case, all partial frequency trajectories would vary in perfect synchronism. In practice, it is observed that the partial frequency trajectories indeed tend to vary together, but factors like instrument characteristics, room acoustics, and reverberation, among others, introduce disturbances that prevent a perfect match between the trajectories. Those disturbances can be modeled as noise, so now  $P_n(t) = n \cdot F_0(t) + N(t)$ , where  $N$  is the noise. If we consider both the fundamental frequency variations  $F_0(t)$  and the noisy disturbances  $N(t)$  as random variables, the lemma applies—in this context,  $A_1$  is the frequency trajectory of a partial of instrument 1, given by the sum of the ideal partial frequency trajectory  $X_1$  and the disturbance  $N_1$ ;  $A_2$  is the frequency trajectory of a partial of instrument 2, which collides with the partial of instrument 1;  $A_3$  is the partial frequency trajectory resulting from the sum of

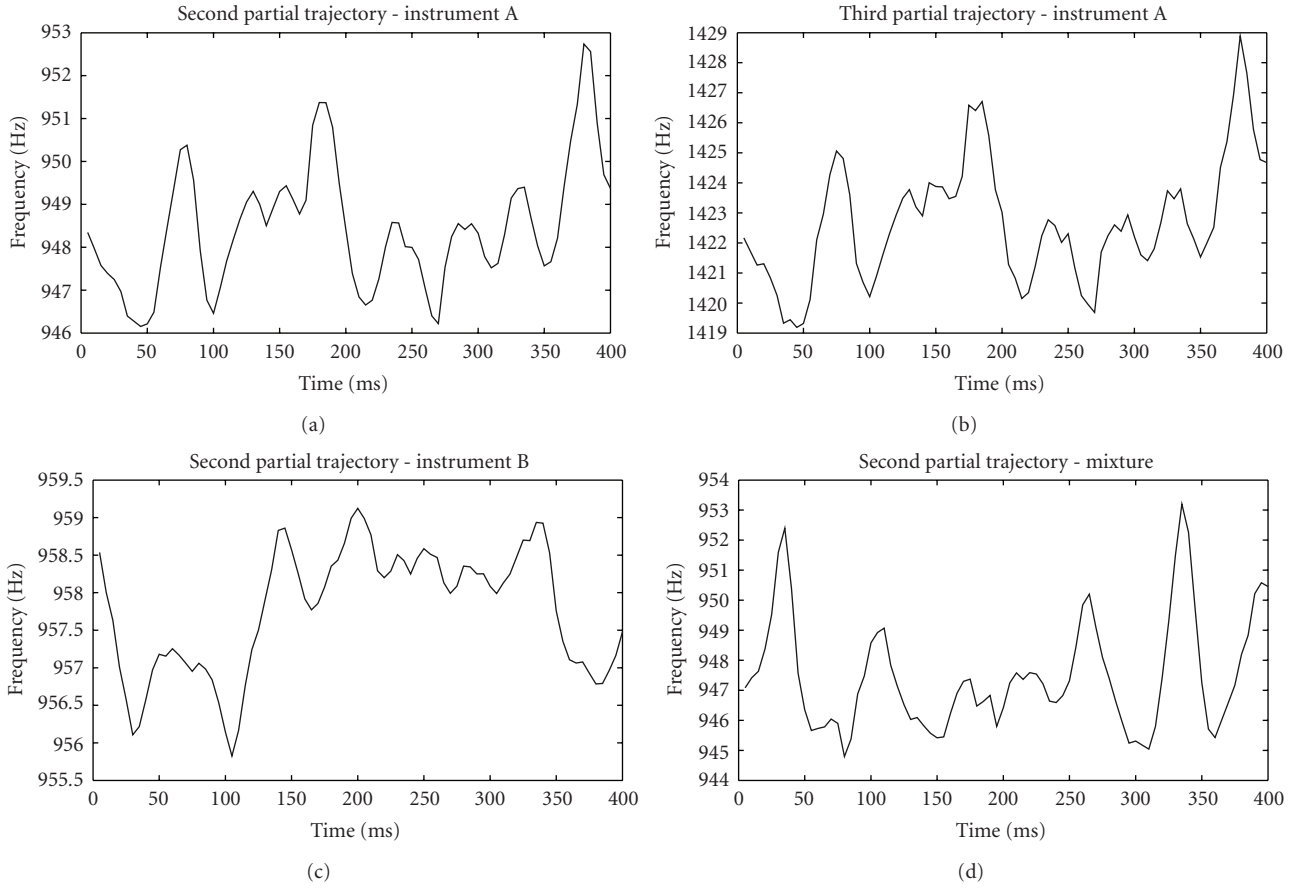


FIGURE 4: Trajectories (a) and (b) come from partials belonging to the same source, thus having very similar behaviors. Trajectory (c) corresponds to a partial from another source. Trajectory (d) corresponds to a mixture partial; its characteristics result from the combination of each partial trends, as well as from phase interactions between the partials. The correlation procedure aims to quantify how close the mixture trajectory is from the behavior expected for each source.

the colliding partials. According to the lemma, the shape of  $A_3$  is the sum of the trajectories  $A_1$  and  $A_2$  weighted by the corresponding amplitudes ( $a$  and  $b$ ). In practice, this assumption holds well when one of the partials has a much larger amplitude than the other one. When the partials have similar amplitudes, the resulting frequency trajectory may differ from the weighted sum. This is not a serious problem because such a difference is normally mild, and the algorithm was designed to explore exactly the cases in which one partial dominates the other ones.

It is important to emphasize that some possible flaws in the model above were not overlooked: there are not many samples to infer the model, the random variables are not IID (independent and identically distributed), and the mixing model is not perfect. However, the lemma and assumptions stated before have as main objective to support the use of cross-correlation to recover the mixing weights, for which purpose they hold sufficiently well—this is confirmed by a number of empirical experiments illustrated in Figures 4 and 5, which show how the correlation varies with respect to the amplitude ratio between the reference source  $A$  and the other sources. Figure 5 was generated using the database described in the beginning of Section 4, in the following way:

- (a) A partial from source  $A$  is taken as reference ( $h_r$ ).
- (b) A second partial of source  $A$  is selected ( $h_a$ ), together with a partial of same frequency from source  $B$  ( $h_b$ ).
- (c) Mixture partials ( $h_m$ ) are generated according to  $w \cdot h_a + (1 - w) \cdot h_b$ , where  $w$  varies between zero and one and represents the dominance of source  $A$ , as represented in the horizontal axis of Figure 5. When  $w$  is zero, source  $A$  is completely absent, and when  $w$  is one, the partial from source  $A$  is completely dominant.
- (d) The correlation values between the frequency trajectories of  $h_r$  and  $h_m$  are calculated and scaled in such a way the normalized correlations are 0 and 1 when  $w = 0$  and  $w = 1$ , respectively. The scaling is performed according to (6), where  $C_{ij}$  is the correlation to be normalized,  $C_{\min}$  is the correlation between the partial from source  $A$  and the mixture when  $w = 0$ , and  $C_{\max}$  is the correlation between the partial from source  $A$  and the mixture when  $w = 1$ —in this case  $C_{\max}$  is always equal to one.

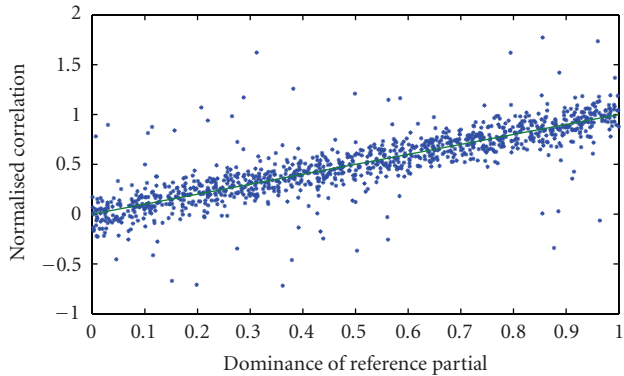


FIGURE 5: Relation between correlation of the frequency trajectories and partial ratio.

If the hypothesis hold perfectly, the normalized correlation would have always the same value of  $w$  (solid line in Figure 5). As can be seen in Figure 5, the hypothesis holds relatively well in most cases; however, there are some instruments (particularly woodwinds) for which this tends to fail. Further investigation will be necessary in order to determine why this happens only for certain instruments. The amplitude estimation procedure described next was designed to mitigate the problems associated to the cases in which the hypotheses tend to fail. As a result, the strategy works fairly well if the hypotheses hold (partially or totally) for at least one of the sources.

The amplitude estimation procedure can be divided into two main parts: determination of reference partials and the actual amplitude estimation, as described next.

**3.4.1. Determination of Reference Partials.** This part of the algorithm aims to find the partials that best represent each source in the mixture. The objective is to find the partials that are less affected by sources other than the one it should represent. The use of reference partials for each source guarantees that the estimated amplitudes within a frame will be correctly grouped. As a result, no intraframe permutation errors can occur. It is important to highlight that this paper is devoted to be problem of estimating the amplitudes for individual frames. A subsequent problem would be taking all frame-wise amplitude estimates within the whole signal and assign them to the correct sources. A solution for this problem based on musical theory and continuity rules is expected to be investigated in the future.

In order to illustrate how the reference partials are determined, consider a hypothetical signal generated by two simultaneous instruments playing the same note. Also, consider that all mixture partials after the fifth have negligible amplitudes. Table 1 shows the frequency correlation values between the partials of this hypothetical signal, as well as the amplitude of each mixture partial. The values between

parentheses are the warped correlation values, calculated according to

$$C'_{ij} = \frac{C_{ij} - C_{\min}}{C_{\max} - C_{\min}}, \quad (6)$$

where  $C_{ij}$  is the correlation value (between partials  $i$  and  $j$ ) to be warped, and  $C_{\min}$  and  $C_{\max}$  are the minimum and maximum correlation values for that frame. As a result, all correlation values now lie between 0 and 1, and the relative differences among the correlation values are reinforced.

The values in Table 1 are used as example to illustrate each step of the procedure to determine the amplitude of each source and partial. Although the example considers mixtures of only two instruments, the rules are valid for any number of simultaneous instruments.

- (a) If a given source has some partials that do not coincide with any other partial, which is determined using the results of the partial positioning procedure described in Section 2.2, the most energetic among such partials is taken as reference for that source. If all sources have at least one of such “clean” partials to be taken as reference, the algorithm skips directly to the amplitude estimation. If at least one source satisfies the “clean partial” condition, the algorithm skips to item (d), and the most energetic reference partial is taken as the global reference partial  $G$ . Items (b) and (c) only take place if no source satisfies such a condition, which is the case of the hypothetical signal.
- (b) The two mixture partials that result in the greatest correlation are selected (first and third in Table 1). Those are the mixture partials for which the frequency variations are more alike, which indicates that they both belong mostly to a same source. In this case, possible coincident partials have small amplitudes compared to the dominant partials.
- (c) The most energetic among those two partials is chosen both as the global reference  $G$  and as reference for the corresponding source, as the partial with greatest amplitude probably has the most defined features to be compared to the remaining ones. In the example given by Table 1, the first partial is taken as reference  $R_1$  for instrument 1 ( $R_1 = 1$ ).
- (d) In this step, the algorithm chooses the reference partials for the remaining sources. Let  $I_G$  be the source of partial  $G$ , and let  $I_C$  be the current source for which the reference partial is to be determined. The reference partial for  $I_C$  is chosen by taking the mixture partial that result in the lowest correlation with respect to  $G$ , provided that the components of such mixture partial belong only to  $I_C$  and  $I_G$  (if no partial satisfies this condition, item (e) takes place). As a result, the algorithm selects the mixture partial in which  $I_C$  is more dominant with respect to  $I_G$ . In the example shown in Table 1, the fourth partial has the lowest correlation with respect to  $G$  ( $-0.3$ ), being taken as reference  $R_2$  for instrument 2 ( $R_2 = 4$ ).

TABLE 1: Illustration of the amplitude estimation procedure. If the last row is removed, the table is a matrix showing the correlations between the mixture partials, and the values between parentheses are the warped correlation values according to (6). Thus, the regular and warped correlations between partials 1 and 2 are, respectively, 0.2 and 0.62. As can be seen, the lowest correlation value overall will have a warped correlation of 0, and the highest correlation value is warped to 1; all other correlations will have intermediate warped value. The last row in the table reveals the amplitude of each one of the mixture partials.

Partial	1	2	3	4	5
1	—	0.2 (0.62)	0.5 (1.0)	-0.3 (0.0)	0 (0.37)
2	—	—	0.1 (0.5)	-0.1 (0.25)	-0.2 (0.12)
3	—	—	—	-0.2 (0.12)	-0.2 (0.12)
4	—	—	—	—	0.1 (0.5)
5	—	—	—	—	—
Amp.	0.7	0.9	0.4	0.5	0.3

- (e) This item takes place if all mixture partials are composed by at least three instruments. In this case, the mixture partial that result in the lowest correlation with respect to  $G$  is chosen to represent the partial least affected by  $I_G$ . The objective now is to remove from the process all partials significantly influenced by  $I_G$ . This is carried out by removing all partials whose warped correlation values with respect to  $R_1$  are greater than half the largest warped correlation value of  $R_1$ . In the example given by Table 1, the largest warped correlation would be 1, and partials 2 and 3 would be removed accordingly. Then, items (a) to (d) are repeated for the remaining partials. If more than two instruments still remain in the process, item (e) takes place once more, and the process continues until all reference partials have been determined.

3.4.2. *Amplitude Estimation.* The reference partials for each source are now used to estimate the relative amplitude to be assigned to each partial of each source, according to

$$A_s(i) = \frac{C'_{i,R_s}}{\sum_{n=1}^N C'_{i,R_n}}, \quad (7)$$

where  $A_s$  indicate the relative amplitude to be assigned to source  $s$  in the mixture partial,  $n$  is the index of the source (considering only the sources that are part of that mixture), and  $C'_{ij}$  is the warped correlation value between partials  $i$  and  $j$ . The warped correlation were used because, as pointed out before, they enhance the relative differences among the correlations. As can be seen in (7), the relative amplitudes to be assigned to the partials in the mixture are directly proportional to the warped correlations of the partial with respect to the reference partials. This reflects the hypothesis that higher correlation values indicate a stronger relative presence of a given instrument in the mixture. Table 2 shows the relative partial amplitudes for the example given by Table 1.

As can be seen, both (6) and (7) are heuristic. They were determined empirically by a thorough observation of the

data and exhaustive tests. Other strategies, both heuristic and statistical, were tested, but this simple approach resulted in a performance comparable to those achieved by more complex strategies.

In the following, the relative partial amplitudes are used to extract the amplitudes of each individual partial from the mixture partial (values between parentheses). In the example, the amplitude of the mixture partial is assumed to be equal to the sum of the amplitudes of the coincident partials. This would only hold if the phases of coincident partials were aligned, which in practice does not occur. Ideally, amplitude and phase should be estimated together to produce accurate estimates. However, the characteristics of the algorithm made it necessary the adoption of simplifications and assumptions that, if uncompensated, might result in inaccurate estimates. To compensate (at least partially) the phase being neglected in previous steps of the algorithm, some further processing is necessary: a rough estimate of which amplitude the mixture would have if the phases were actually perfectly aligned is obtained by summing the amplitudes estimated using part of the algorithm proposed by Yeh and Roebel [42] in Sections 2.1 and 2.2 of their paper. This rough estimate is, in general, larger than the actual amplitude of the mixture partial. This difference between both amplitudes is a rough measure of the phase displacement between the partials. To compensate for such a phase displacement, a weighting factor given by  $w = A_r/A_m$ , where  $A_r$  is the rough amplitude estimate and  $A_m$  is the actual amplitude of the mixture partial and is multiplied to the initial zero-phase partial amplitude estimates. This procedure improves the accuracy of the estimates by about 10%.

As a final remark, it is important to emphasize that the amplitudes within a frame are not constant. In fact, the proposed method explores the frequency modulation (FM) of the signals, and FM is often associated with some kind of amplitude modulation (AM). However, the intraframe amplitude variations are usually small (except in some cases of strong vibrato), making it reasonable to estimate an average amplitude instead of detecting the exact amplitude envelope, which would be a task close to impossible.

TABLE 2: Relative and corresponding effective partial amplitudes (between parentheses). The relative amplitudes reveal which percentage of the mixture partial should be assigned to each source, hence the sum in each column is always 1 (100%). The effective amplitudes are obtained by multiplying the relative amplitudes by the mixture partial amplitudes shown in the last row of Table 1, hence the sum of each column in this case is equal to the amplitudes shown in the last row of Table 1.

Partial	1	2	3	4	5
Inst. 1	1 (0.7)	0.71 (0.64)	0.89 (0.36)	0 (0)	0.43 (0.13)
Inst. 2	0 (0)	0.29 (0.26)	0.11 (0.04)	1 (0.5)	0.57 (0.17)

## 4. Experimental Results

The mixtures used in the tests were generated by summing individual notes taken from the instrument samples present in the RWC database [43]. Eighteen instruments of several types (winds, bowed strings, plucked strings, and struck strings) were considered—mixtures including both vocals and instruments were tested separately, as described in Section 4.7. In total, 40156 mixtures of two instruments, three, four and five instruments were used in the tests. The mixtures of two sources are composed by instruments playing in unison (same note), and the other mixtures include different octave relations (including unison). A mixture can be composed by the same kind of instrument. Those settings were chosen in order to test the algorithm with the hardest possible conditions. All signals are sampled at 44.1 kHz, and have a minimum duration of 800 ms. Next subsections present the main results according to different performance aspects.

**4.1. Overall Performance and Comparison with Interpolation Approach.** Table 3 shows the mean RMS amplitude error resulting from the amplitude estimation of the first 12 partials in mixtures with two to five instruments (I2 to I5 in the first column). The error is given in dB and is calculated according to

$$\text{error} = \frac{E_{\text{abs}}}{A_{\text{max}}}, \quad (8)$$

where  $E_{\text{abs}}$  is the absolute error between the estimate and the correct amplitude, and  $A_{\text{max}}$  is the amplitude of the most energetic partial. The error values for the interpolation approach were obtained by taking an individual instrument playing a single note, and then measuring the error between the estimate resulting from the interpolation of the neighbor partials and the actual value of the partial. This represents the ideal condition for the interpolation approach, since the partials are not disturbed at all by other sources. The inherent dependency of the interpolation approach on clean partials makes its use very limited in real situations, especially if several instruments are present. This must be taken into consideration when comparing the results in Table 3.

In Table 3, the partial amplitudes of each signal were normalized so the most energetic partial has a RMS value equal to 1. No noise besides that naturally occurring in the recordings was added, and the RMS values of the sources have a 1 : 1 ratio.

The results for higher partials are not shown in Table 3 in order to improve the legibility of the results. Additionally,

their amplitudes are usually small, and so is their absolute error, thus including their results would not add much information. Finally, due to the rules defined in Section 2.2, normally only a few partials above the twelfth are considered. As a consequence, higher partials will have much less results to be averaged, thus their results are less significant. Only one line was dedicated to the interpolation approach because the ideal conditions adopted in the tests make the number of instruments in the mixture irrelevant.

The total errors presented in Table 3 were calculated taking only the 12 first partials into consideration. The remaining partials were not considered because their only effect would be reducing the total error value.

Before comparing the techniques, there are some important remarks to be made about the results shown in Table 3. As can be seen, for both techniques the mean errors are smaller for higher partials. This is not because they are more effective in those cases, but because the amplitudes of higher partials tend to be smaller, and so does the error, since it is calculated having the most energetic partial as reference. As a response, new error rates—called modified mean error—were calculated for two-instrument mixtures using as reference the average amplitude of the partials, as shown in Table 4—the error values for the other mixtures were omitted because they have approximately the same behavior. The modified errors are calculated as in (8), but in this case  $A_{\text{max}}$  is replaced by the average amplitude of the 12 partials.

As stated before, the results for the interpolation approach were obtained under ideal conditions. Also, it is important to note that the first partial is often the most energetic one, resulting in greater absolute errors. Since the interpolation procedure cannot estimate the first partial, it is not part of the total error. In real situations with different kinds of mixtures present, the results for the interpolation approach could be significantly worse. As can be seen in Table 3, although facing harder conditions, the proposed strategy outperforms the interpolation approach even when dealing with several simultaneous instruments. This indicates that the relative improvement achieved by the proposed algorithm with respect to the interpolation method is significant.

As expected, the best results were achieved for mixtures of two instruments. The accuracy degrades when more instruments are considered, but meaningful estimates can be obtained for up to five simultaneous instruments. Although the algorithm can, in theory, deal with mixtures of six or more instruments, in such cases the spectrum tends to become too crowded for the algorithm to work properly.

TABLE 3: Mean error comparison between the proposed algorithm and the interpolation approach (in dB).

Partial	1	2	3	4	5	6	7	8	9	10	11	12	Total
I2	-7.1	-8.5	-9.7	-11.2	-12.3	-13.7	-14.8	-15.9	-17.0	-17.5	-18.3	-19.2	-12.0
I3	-5.4	-6.7	-7.9	-9.4	-10.3	-11.9	-12.8	-13.9	-14.8	-15.6	-16.2	-17.0	-10.2
I4	-4.8	-6.1	-7.4	-8.8	-9.9	-11.2	-12.4	-13.4	-14.1	-15.0	-15.6	-16.0	-9.6
I5	-4.5	-5.8	-7.0	-8.4	-9.5	-10.8	-12.0	-12.9	-13.6	-14.5	-14.8	-15.2	-9.2
Interp.	<sup>a</sup>	-4.6	-6.2	-7.7	-8.9	-9.9	-10.3	-10.6	-11.0	-10.8	-10.5	-10.5	-8.6

<sup>a</sup>First partial cannot be estimated.

TABLE 4: Modified mean error values in dB.

Partial	1	2	3	4	5	6	7	8	9	10	11	12	Total
Prop.	-5.4	-5.3	-5.8	-5.9	-6.0	-6.1	-6.4	-6.3	-6.6	-6.4	-6.6	-6.8	-6.1

Analyzing specifically Table 4, it can be observed that the performance of the proposed method is slightly better for higher partials.

This is because the mixtures in Table 4 were generated using instruments playing the same notes, and higher partials in that kind of mixture are more likely to be strongly dominated by one of the instruments—most instruments have strong low partials, so they will all have significant contributions in the lower partials of the mixture. Mixture partials that are strongly dominated by a single instrument normally result in better amplitude estimates, because they correlate well with the reference partials, explaining the results shown in Table 4.

From this point to the end of Section 4, all results were obtained using two-instrument mixtures—other mixtures were not included to avoid redundancy.

**4.2. Performance Under Noisy Conditions.** Table 5 shows the performance of the proposal when the signals are corrupted by additive white noise. The results were obtained by artificially summing the white noise to the mixtures of two signals used in Section 4.1.

As can be seen, the performance is only weakly affected by noise. The error rates only begin to rise significantly close to 0 dB but, even under such an extremely noisy condition, the error rate is only 25% greater than that achieved without any noise. Such a remarkable robustness to noise probably happens because, although noise introduces a random factor in the frequency tracking described in Section 3.2, the frequency variation tendencies are still able to stand out.

**4.3. Influence of RMS Ratio.** Table 6 shows the performance of the proposal for different RMS ratios between the sources. The signals were generated as described in Section 4.1, but scaling one of the sources to result in the RMS ratios shown in Table 6. As can be seen, the RMS ratio between the sources has little impact on the performance of the strategy.

**4.4. Length of the Frames.** As stated in Section 2.1, the best way to get the most reliable results is to divide the signal in

frames with variable lengths according to the occurrence of onsets. Therefore, it is useful to determine how dependent the performance is to the frame length. Table 7 shows the results for different fixed frame lengths. The signals were generated by simply taking the two-partial mixtures used in Section 4.1 and truncating the frames to the lengths shown in Table 7.

As expected, the performance degrades as shorter frames are considered because there is less information available, making the estimates less reliable. The interpolation results are affected in almost the same way, which indicates that this is indeed a matter of lack of information, and not a problem related to the characteristics of the algorithm. Future algorithm improvements may include a way of exploring the information contained in other frames to counteract the damaging effects of using short frames.

**4.5. Onset Errors.** This section analyses the effects of onset misplacements. The following kinds of onset location errors may occur.

- (a) Small errors: errors smaller than 10% of the frame length have little impact in the accuracy of the amplitude estimates. If the onset is placed after the actual position, a small section of the actual frame will be discarded, in which case there is virtually no loss. If the onset is placed before the actual position, a small section of other note may be considered, slightly affecting the correlation values. This kind of mistake increases the amplitude estimation error in about 2%.
- (b) Large errors, estimated onset placed after the actual position: the main consequence of this kind of mistake is that fewer points are available in the calculation of the correlations, which has a relatively mild impact in the accuracy. For instruments whose notes decay with time, like piano and guitar, a more damaging consequence is that the most relevant part of the signal may not be considered in the frame. The main problem here is that after the note decays by a certain amount, the frequency fluctuations in different partials may begin to decorrelate. Therefore,

TABLE 5: Mean error values in dB for different noise levels.

SNR (dB)	60+	50	40	30	20	10	0
Error (dB)	-12.0	-12.0	-12.0	-12.0	-11.9	-11.8	-11.0

TABLE 6: Mean error in dB for different RMS ratios.

Ratio	1 : 1	1 : 0.9	1 : 0.7	1 : 0.5	1 : 0.3
Error (dB)	-12.0	-12.0	-12.0	-12.2	-11.8

TABLE 7: Mean error in dB for different frame lengths.

Length (s)	1	0.5	0.2	0.1
Proposal	-12.0	-11.7	-11.3	-10.8
Interpol.	-8.6	-8.4	-8.0	-7.6

if the strongest part of the note is not considered, the results tend to be worse. Figure 6 shows the dependency of the RMSE values on the extent of the onset misplacements. The results shown in the figure were obtained exactly in the same way as those in Section 4.1, but deliberately misplacing the onsets to reveal the effects of this kind of error.

- (c) Large errors, estimated onset placed before the actual position: in this case, a part of the signal that does not contain the new note is considered. The effect of this kind of error is that many points that should not be considered in the correlation calculation are taken into account. As can be seen in Figure 6, the larger is the error, the worse is the amplitude estimate.

There are other kinds of onset errors besides positioning—missing and spurious onsets. The analysis of those kinds of errors is analog to that presented to the onset location errors. The effect of spurious onset is that the note will be divided into additional segments, so there will be fewer points available for the calculation, and the observations presented in item (b) hold. In the case of missing onset, two segments containing different notes will be considered, in a situation that is similar to that discussed in item (c).

**4.6. Impact of Lower Octave Errors.** As stated in Section 2.2, lower octave errors may affect the accuracy of the proposed algorithm when this is cascaded with a F0 estimator. Table 8 shows the algorithm accuracy for the actual partials when the estimated F0 for one of them is one, two or three octaves below the actual value. As commented before, the lower octave errors usually introduce a number of low correlations that are mistakenly taken into account in the amplitude estimation procedure described in Section 3.4. Since the choice of the first reference partial is based on the highest correlation, it is not usually affected by the lower octave error. If this first reference partial belongs to the instrument for which the fundamental frequency was misestimated, the choice of the other reference partial will also not be affected, because in this case all potential partials actually belong to the instrument. Also, all correlations considered in this case

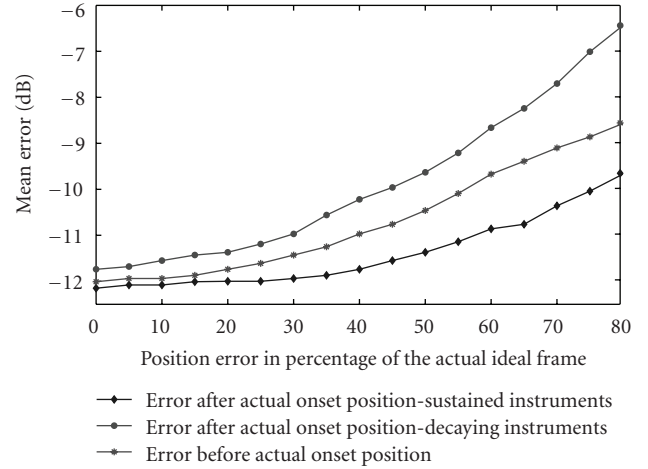


FIGURE 6: Impact of onset misplacements in the accuracy of the proposed algorithm.

are valid, as they are related to the first reference partial. As a result, the accuracy of amplitude estimates is not affected.

Problems occur when the first reference partial belongs to the instrument whose F0 was correctly estimated. In this case, several false potential partials will be considered in the process to determine the second reference partial, which is chosen based on the lowest correlation. Since those false partials are expected to have very low correlations with respect to all other partials, the chance of one of them being taken as reference is high. In this case, all the process is disrupted and the amplitude estimates are likely to be wrong. This explains the deterioration of the results shown in Table 8. Those observations can be extended to mixtures with any number of instruments, and the higher is the number of F0 misestimates, the worse will be the results.

**4.7. Separating Vocals.** The mixtures used in this section were generated by taking vocal samples from the RWC instrument database [43] and adding an accompanying instrument or another vocal. Therefore, all mixtures are composed by two sources, with at least one being a vocal sample. Several notes of all 18 instruments were considered, and they were all scaled to have the same RMS value as the vocal sample. Table 9 shows the results when the algorithm was applied to separate vocals from the accompanying instruments (second row) and from other vocals (third row). The vocals were produced by male and female adults with different pitch ranges (soprano, alto, tenor, baritone and bass), and consist of vowels being verbalized in a sustained way.

The results shown in Table 9 refer only to the vocal sources, and the conditions are the same as those used to generate Table 3.

TABLE 8: Mean error in dB for some lower octave errors.

Partial	1	2	3	4	5	6	7	8	9	10	11	12	Total
no error	-7.1	-8.5	-9.7	-11.2	-12.2	-13.6	-14.8	-15.9	-17.1	-17.3	-18.2	-18.2	-12.0
1 octave	-5.9	-7.3	-8.5	-10.1	-11.1	-12.5	-13.6	-14.7	-15.9	-15.9	-17.1	-17.3	-10.8
2 octaves	-5.3	-6.7	-7.9	-9.5	-10.4	-11.9	-13.1	-14.1	-15.5	-15.4	-16.4	-16.3	-10.4
3 octaves	-4.8	-6.2	-7.3	-9.1	-9.9	-11.4	-12.5	-13.6	-14.9	-14.9	-15.7	-15.9	-9.8

TABLE 9: Mean error in dB for vocal signals.

Partial	1	2	3	4	5	6	7	8	9	10	11	12	Total
V × I	-7.2	-8.2	-9.9	-11.2	-12.5	-13.5	-13.9	-14.3	-14.3	-14.2	-14.2	-14.3	-11.5
V × V	-6.9	-7.9	-9.6	-10.8	-11.9	-13.0	-13.2	-13.8	-13.6	-13.5	-13.5	-13.6	-11.1

As can be seen, the results for vocal sources are only slightly worse than those achieved for musical instruments. This indicates that the algorithm is also suitable for dealing with vocal signals. Future work will try to extend the technique to the speech separation problem.

*4.8. Final Remarks.* The problem of estimating the amplitude of coincident partials is a very difficult one. More than that, this is a technology in its infancy. In that context, many of the solutions adopted did not perform perfectly, and there are some pathological cases in which the method tends to fail completely. However, the algorithm performs reasonably well in most cases, which shows its potentiality. Since this is a technology far from mature, each part of the algorithm will probably be under scrutiny in the near future. The main motivation for this paper was to propose a completely different way of tackling the problem of amplitude estimation, highlighting its strong characteristics and pointing out the aspects that still need improvement. In short, this paper was intended to be a starting point in the development of a new family of algorithms capable of overcoming some of the main difficulties currently faced by both amplitude estimation and sound source separation algorithms.

## 5. Conclusions

This paper presented a new strategy to estimate the amplitudes of coincident partials. The proposal has several advantages over its predecessors, such as better accuracy, the ability to estimate the first partial, reliable estimates even if the instruments are playing the same note, and so forth. Additionally, the strategy is robust to noise and is able to deal with any number of simultaneous instruments.

Although it presents a better performance than its predecessor, there is still room for improvement. Future versions may include new procedures to refine the estimates, like using the information from previous frames to verify the consistency of the current estimates. The extension of the technique to the speech separation problem is currently under investigation.

## Appendix

### Proof of Lemma 1

Let  $A_1 = X_1 + N_1$  and  $A_2 = X_2 + N_2$ , where  $X_1$  and  $X_2$  are random variables representing the actual partial frequency trajectory, and  $N_1$  and  $N_2$  are random variables representing the zero-mean, independent noise associated. Then,  $A_3 = aA_1 + bA_2 = aX_1 + bX_2 + aN_1 + bN_2$  and

$$\rho_{A_1, A_3} = \frac{E(A_1 A_3) - E(A_1)E(A_3)}{\sigma_{A_1} \sigma_{A_3}} \quad (\text{A.1})$$

$$\rho_{A_2, A_3} = \frac{\sigma_{A_2} \sigma_{A_3}}{E(A_2 A_3) - E(A_2)E(A_3)},$$

In the following, each term of (A.1) is expanded:

$$E(A_1 \cdot A_3) = E[(X_1 + N_1) \cdot (aX_1 + bX_2 + aN_1 + bN_2)]$$

$$= aE(X_1^2) + bE(X_1)E(X_2) + aE(N_1^2). \quad (\text{A.2})$$

The terms  $aE^2(X_1)$  and  $aE^2(N_1)$  are then summed and subtracted to the expression, keeping it unaltered. This is done to explore the relation  $\sigma_X^2 = E(X^2) - E^2(X)$  and, assuming that  $E(N_1) = 0$  and  $E(N_2) = 0$ , the expression becomes

$$E(A_1 \cdot A_3) = aE(X_1^2) + bE(X_1)E(X_2) + aE(N_1^2)$$

$$+ \underbrace{aE^2(X_1) - aE^2(X_1)}_{=0} + \underbrace{aE^2(N_1) - aE^2(N_1)}_{=0}$$

$$= aE(X_1^2) - aE^2(X_1) + bE(X_1)E(X_2) + aE(N_1^2)$$

$$- aE^2(N_1) + \underbrace{aE^2(N_1)}_{=0} + aE^2(X_1)$$

$$= a\sigma_{X_1}^2 + bE(X_1)E(X_2) + a\sigma_{N_1}^2 + aE^2(X_1). \quad (\text{A.3})$$

Following the same steps,

$$E(A_2 \cdot A_3) = b\sigma_{X_2}^2 + aE(X_1)E(X_2) + b\sigma_{N_2}^2 + bE^2(X_2). \quad (\text{A.4})$$

The other terms are given by

$$\begin{aligned} E(A_1) \cdot E(A_3) &= E(X_1)(aE(X_1) + bE(X_2)) \\ &= aE^2(X_1) + bE(X_1)E(X_2), \\ E(A_2) \cdot E(A_3) &= E(X_2)(aE(X_1) + bE(X_2)) \\ &= bE^2(X_2) + aE(X_1)E(X_2). \end{aligned} \quad (\text{A.5})$$

Substituting all these terms in (A.1) and eliminating self-cancelling terms, the expression becomes

$$\frac{\rho_{A_1,A_3}}{\rho_{A_2,A_3}} = \frac{a \cdot (\sigma_{X_1}^2 + \sigma_{N_1}^2)}{b \cdot (\sigma_{X_2}^2 + \sigma_{N_2}^2)} \cdot \frac{\sigma_{A_2}}{\sigma_{A_1}}. \quad (\text{A.6})$$

Considering that  $\sigma_{A_1}^2 = \sigma_{X_1}^2 + \sigma_{N_1}^2$  and  $\sigma_{A_2}^2 = \sigma_{X_2}^2 + \sigma_{N_2}^2$ , then

$$\frac{\rho_{A_1,A_3}}{\rho_{A_2,A_3}} = \frac{a \cdot (\sigma_{X_1}^2 + \sigma_{N_1}^2)}{b \cdot (\sigma_{X_2}^2 + \sigma_{N_2}^2)} \cdot \frac{\sqrt{\sigma_{X_2}^2 + \sigma_{N_2}^2}}{\sqrt{\sigma_{X_1}^2 + \sigma_{N_1}^2}}. \quad (\text{A.7})$$

If  $\sigma_{N_1}^2 \ll \sigma_{X_1}^2$  and  $\sigma_{N_2}^2 \ll \sigma_{X_2}^2$ , then

$$\frac{\rho_{A_1,A_3}}{\rho_{A_2,A_3}} = \frac{a}{b} \cdot \frac{\sigma_{X_1}^2}{\sigma_{X_2}^2} \cdot \frac{\sigma_{X_2}}{\sigma_{X_1}} = \frac{a}{b} \cdot \frac{\sigma_{X_1}}{\sigma_{X_2}}. \quad (\text{A.8})$$

Additionally if  $\sigma_{X_1} \equiv \sigma_{X_2}$ ,

$$\frac{\rho_{A_1,A_3}}{\rho_{A_2,A_3}} = \frac{a}{b}. \quad (\text{A.9})$$

## Acknowledgments

Special thanks are extended to Foreign Affairs and International Trade Canada for supporting this work under its Post-Doctoral Research Fellowship Program (PDRF). The authors also would like to thank Dr. Sudhakar Ganti for his help. Work was performed while the first author was with the Department of Computer Science, University of Victoria, Canada.

## References

- [1] K. Kokkinakis and A. K. Nandi, "Multichannel blind deconvolution for source separation in convolutive mixtures of speech," *IEEE Transactions on Audio, Speech and Language Processing*, vol. 14, no. 1, pp. 200–212, 2006.
- [2] H. Saruwatari, T. Kawamura, T. Nishikawa, A. Lee, and K. Shikano, "Blind source separation based on a fast-convergence algorithm combining ICA and beamforming," *IEEE Transactions on Audio, Speech and Language Processing*, vol. 14, no. 2, pp. 666–678, 2006.
- [3] T. Kim, H. T. Attias, S.-Y. Lee, and T.-W. Lee, "Blind source separation exploiting higher-order frequency dependencies," *IEEE Transactions on Audio, Speech and Language Processing*, vol. 15, no. 1, pp. 70–79, 2007.
- [4] S. C. Douglas, M. Gupta, H. Sawada, and S. Makino, "Spatio-temporal FastICA algorithms for the blind separation of convolutive mixtures," *IEEE Transactions on Audio, Speech and Language Processing*, vol. 15, no. 5, pp. 1511–1520, 2007.
- [5] N. Roman and D. Wang, "Pitch-based monaural segregation of reverberant speech," *Journal of the Acoustical Society of America*, vol. 120, no. 1, pp. 458–469, 2006.
- [6] Ö. Yilmaz and S. Rickard, "Blind separation of speech mixtures via time-frequency masking," *IEEE Transactions on Signal Processing*, vol. 52, no. 7, pp. 1830–1846, 2004.
- [7] M. H. Radfar and R. M. Dansereau, "Single-channel speech separation using soft mask filtering," *IEEE Transactions on Audio, Speech and Language Processing*, vol. 15, no. 8, pp. 2299–2310, 2007.
- [8] R. Saab, Ö. Yilmaz, M. J. McKeown, and R. Abugharbieh, "Underdetermined anechoic blind source separation via  $\ell^q$ -basis-pursuit With  $q \ll 1$ ," *IEEE Transactions on Signal Processing*, vol. 55, no. 8, pp. 4004–4017, 2007.
- [9] A. Aïssa-El-Bey, N. Linh-Trung, K. Abed-Meraim, A. Belouchrani, and Y. Grenier, "Underdetermined blind separation of non-disjoint sources in the time-frequency domain," *IEEE Transactions on Signal Processing*, vol. 55, no. 3, pp. 897–907, 2007.
- [10] A. Aïssa-El-Bey, K. Abed-Meraim, and Y. Grenier, "Blind separation of underdetermined convolutive mixtures using their time-frequency representation," *IEEE Transactions on Audio, Speech and Language Processing*, vol. 15, no. 5, pp. 1540–1550, 2007.
- [11] M. K. I. Molla and K. Hirose, "Single-mixture audio source separation by subspace decomposition of hilbert spectrum," *IEEE Transactions on Audio, Speech and Language Processing*, vol. 15, no. 3, pp. 893–900, 2007.
- [12] A. Abramson and I. Cohen, "Single-sensor audio source separation using classification and estimation approach and GARCH modeling," *IEEE Transactions on Audio, Speech and Language Processing*, vol. 16, no. 8, pp. 1528–1540, 2008.
- [13] Y. Li and D. Wang, "Separation of singing voice from music accompaniment for monaural recordings," *IEEE Transactions on Audio, Speech and Language Processing*, vol. 15, no. 4, pp. 1475–1487, 2007.
- [14] T. Virtanen, "Monaural sound source separation by non-negative matrix factorization with temporal continuity and sparseness criteria," *IEEE Transactions on Audio, Speech and Language Processing*, vol. 15, no. 3, pp. 1066–1074, 2007.
- [15] L. Benaroya, F. Bimbot, and R. Gribonval, "Audio source separation with a single sensor," *IEEE Transactions on Audio, Speech and Language Processing*, vol. 14, no. 1, pp. 191–199, 2006.
- [16] T. Tolonen, "Methods for separation of harmonic sound sources using sinusoidal modeling," in *Proceedings of the Audio Engineering Society Convention*, May 1999, preprint 4958.
- [17] K. Itoyama, M. Goto, K. Komatani, T. Ogata, and H. G. Okuno, "Integration and adaptation of harmonic and inharmonic models for separating polyphonic musical signals," in *Proceedings of IEEE International Conference on Acoustics, Speech and Signal Processing (ICASSP '07)*, pp. 57–60, April 2007.
- [18] L. Benaroya, L. M. Donagh, F. Bimbot, and R. Gribonval, "Non negative sparse representation for Wiener based source separation with a single sensor," in *Proceedings of IEEE International Conference on Acoustics, Speech, and Signal Processing (ICASSP '03)*, pp. 613–616, April 2003.
- [19] J. J. Burred and T. Sikora, "On the use of auditory representations for sparsity-based sound source separation," in *Proceedings of the 5th International Conference on Information, Communications and Signal Processing*, pp. 1466–1470, December 2005.

- [20] Z. He, S. Xie, S. Ding, and A. Cichocki, "Convolutional blind source separation in the frequency domain based on sparse representation," *IEEE Transactions on Audio, Speech and Language Processing*, vol. 15, no. 5, pp. 1551–1563, 2007.
- [21] M. Ito and M. Yano, "Sinusoidal modeling for nonstationary voiced speech based on a local vector transform," *Journal of the Acoustical Society of America*, vol. 121, no. 3, pp. 1717–1727, 2007.
- [22] J. McAulay and T. F. Quatieri, "Speech analysis/synthesis based on a sinusoidal representation," *IEEE Transactions on Acoustics, Speech, and Signal Processing*, vol. 34, no. 4, pp. 744–754, 1986.
- [23] J. O. Smith and X. Serra, "PARSHL: an analysis/synthesis program for non-harmonic sounds based on a sinusoidal representation," in *Proceedings of the International Computer Music Conference (ICMC '87)*, pp. 290–297, 1987.
- [24] X. Serra, "Musical sound modeling with sinusoids plus noise," in *Musical Signal Processing*, C. Roads, S. Pope, A. Picialli, and G. D. Poli, Eds., pp. 91–122, Swets & Zeitlinger, 1997.
- [25] T. Virtanen, *Sound source separation in monaural music signals*, Ph.D. dissertation, Tampere University of Technology, Finland, 2006.
- [26] A. Klapuri, T. Virtanen, and J.-M. Holm, "Robust multipitch estimation for the analysis and manipulation of polyphonic musical signals," in *Proceedings of the COST-G6 Conference on Digital Audio Effects*, pp. 141–146, 2000.
- [27] T. Virtanen and A. Klapuri, "Separation of harmonic sounds using linear models for the overtone series," in *Proceedings of IEEE International Conference on Acoustics, Speech and Signal Processing (ICASSP '02)*, pp. 1757–1760, May 2002.
- [28] M. R. Every and J. E. Szymanski, "Separation of synchronous pitched notes by spectral filtering of harmonics," *IEEE Transactions on Audio, Speech and Language Processing*, vol. 14, no. 5, pp. 1845–1856, 2006.
- [29] H. Viste and G. Evangelista, "A method for separation of overlapping partials based on similarity of temporal envelopes in multichannel mixtures," *IEEE Transactions on Audio, Speech and Language Processing*, vol. 14, no. 3, pp. 1051–1061, 2006.
- [30] Z. Duan, Y. Zhang, C. Zhang, and Z. Shi, "Unsupervised single-channel music source separation by average harmonic structure modeling," *IEEE Transactions on Audio, Speech and Language Processing*, vol. 16, no. 4, pp. 766–778, 2008.
- [31] J. Woodruff, Y. Li, and D. L. Wang, "Resolving overlapping harmonics for monaural musical sound separation using pitch and common amplitude modulation," in *Proceedings of the International Conference on Music Information Retrieval*, pp. 538–543, 2008.
- [32] J. J. Burred and T. Sikora, "Monaural source separation from musical mixtures based on time-frequency timbre models," in *Proceedings of the International Conference on Music Information Retrieval*, pp. 149–152, 2007.
- [33] R. C. Maher, "Evaluation of a method for separating digitized duet signals," *Journal of the Audio Engineering Society*, vol. 38, no. 12, pp. 956–979, 1990.
- [34] T. Virtanen and A. Klapuri, "Separation of harmonic sound sources using sinusoidal modeling," in *Proceedings of IEEE International Conference on Acoustics, Speech, and Signal Processing (ICASSP '00)*, pp. 765–768, June 2000.
- [35] M. Gainza, B. Lawlor, and E. Coyle, "Harmonic sound source separation using FIR comb filters," in *Proceedings of the Audio Engineering Society Convention*, 2004, preprint 6312.
- [36] H. Thornburg, R. J. Leistikow, and J. Berger, "Melody extraction and musical onset detection via probabilistic models of framewise STFT peak data," *IEEE Transactions on Audio, Speech and Language Processing*, vol. 15, no. 4, pp. 1257–1272, 2007.
- [37] G. Hu and D. Wang, "Auditory segmentation based on onset and offset analysis," *IEEE Transactions on Audio, Speech and Language Processing*, vol. 15, no. 2, pp. 396–405, 2007.
- [38] A. Klapuri, "Multiple fundamental frequency estimation by summing harmonic amplitudes," in *Proceedings of the International Conference on Music Information Retrieval*, pp. 216–221, 2006.
- [39] J. Rauhala, H.-M. Lehtonen, and V. Välimäki, "Fast automatic inharmonicity estimation algorithm," *Journal of the Acoustical Society of America*, vol. 121, no. 5, pp. EL184–EL189, 2007.
- [40] J. C. Brown, "Frequency ratios of spectral components of musical sounds," *Journal of the Acoustical Society of America*, vol. 99, no. 2, pp. 1210–1218, 1996.
- [41] M. Wu, D. L. Wang, and G. J. Brown, "A multipitch tracking algorithm for noisy speech," *IEEE Transactions on Speech and Audio Processing*, vol. 11, no. 3, pp. 229–241, 2003.
- [42] C. Yeh and A. Roebel, "The expected amplitude of overlapping partials of harmonic sounds," in *2009 IEEE International Conference on Acoustics, Speech, and Signal Processing (ICASSP '09)*, pp. 3169–3172, twN, April 2009.
- [43] M. Goto, "Development of the RWC music database," in *Proceedings of the 18th International Congress on Acoustics (ICA '04)*, pp. 553–556, 2004.